



EVALUATION OF SPINAL DYSRAPHISM BY MRI

Radiology

**Manisha
Narayanbhai
Solanki**

Associate Professor, Department of Radiology, GMERS Medical College & Hospital, Sola, Ahmedabad, Gujarat, India

**Vasantkumar
Jethabhai Rathod***

Assistant Professor, Department of Radiology, B.J. Medical College & Civil Hospital, Ahmedabad, Gujarat, India*Corresponding Author

ABSTRACT

BACKGROUND: Spinal dysraphism is one of the most common congenital disorders associated with significant morbidity and mortality. MRI is the dominant modality in use for spinal dysraphism. Aim of this study was to know relative frequency of different types of spinal dysraphism & to know their MR appearances. **MATERIAL & METHOD:** This prospective study was done in our institute B.J. Medical College & Civil Hospital, Ahmedabad, Gujarat, India. It included 100 cases of spinal dysraphism which had undergone MRI examination from January 2024 to October 2025. **RESULTS:** In our study, Maximum patients were in the age group 0-10 yrs. M:F ratio was 1:1.22. Most common type of spinal dysraphism was Myelomeningocele. Most common site of spinal dysraphism was lumbosacral region. **CONCLUSION:** Myelomeningocele is the most common type of spinal dysraphism. MRI allows for the delineation of the spinal cord, subarachnoid space, vertebral bodies, posterior elements, intervertebral discs & other soft tissues. MRI plays a pivotal role in diagnosis and presurgical evaluation of spinal dysraphism.

KEYWORDS

Spinal dysraphism, Magnetic resonance imaging (MRI).

INTRODUCTION:

Spinal dysraphism is one of the most common congenital disorders associated with significant morbidity and mortality. They are second most common congenital anomaly after congenital heart disease. Estimated prevalence of spinal dysraphism in world is about one to three per 1000 live birth. Most common Neural tube defect in developing countries like India is spinal dysraphism. The incidence varies from 0.5-11 per 1000 live births in different parts of India. Most common site for developmental anomalies of spine is lumbosacral spine, involved in 90% of cases, followed by the thoracic spine (6%–8%) and cervical spine (2%–4%). In last few decades, improved antenatal care, better nutrition for women, and folic acid supplementation have all contributed to a decline in the prevalence of spinal dysraphism around the world. MRI is the mainstay modality in use for spinal dysraphism. MRI is useful in pre-operative assessment of spinal dysraphism cases. Aim of this study was to know relative frequency of different types of spinal dysraphism & to know their MR appearances.

MATERIAL & METHOD:

Study type: Prospective study

Study period: January 2024 to October 2025

Study setting: Department of Radiology, B.J. Medical College & Civil Hospital, Ahmedabad, Gujarat, India.

Sample size: 100 patients

Study procedure:

Study included 100 cases of spinal dysraphism whose MRI was done in our department. MRI were done using Siemens Sempra 1.5 T MRI scanner. All patients underwent plain MRI of spine along with plain MRI of brain under sedation. Each patient was studied in detail with relevant clinical history and clinical examination findings.

RESULTS:

After analysis of data of 100 patients, following results were obtained.

TABLE 1: CASES OF OPEN SPINAL DYSRAPHISM

Sr. No.	Type	Number of cases	Percentage	
			(Out of 100)	(Out of 65)
1.	Myelomeningocele	64	64%	98.46%
2.	Myelocele	1	1%	1.53%
	Total	65	65%	100%

TABLE 2: CASES OF CLOSED SPINAL DYSRAPHISM

Sr. No.	Type	Number of cases	Percentage	
			(Out of 100)	(Out of 35)
1.	Spinal lipomas	16	16%	45.71%
2.	Diastematomyelia	3	3%	8.57%
3.	Dorsal dermal sinus	6	6%	17.14%
4.	Meningocele	6	6%	17.14%
5.	Anterior sacral Meningocele	3	3%	8.57%
6.	Sacral agenesis	1	1%	2.85%
	Total	35	35%	100%

TABLE 3: SPINAL LIPOMAS

Type	Number of cases	Percentage
Lipomyelocele	4	25%
Lipomyelomeningocele	10	62.5%
Dural lipoma	0	0%
Filar lipoma	2	12.5%
Total	16	100%

TABLE 4: CUTANEOUS MANIFESTATIONS OF CLOSED SPINAL DYSRAPHISM

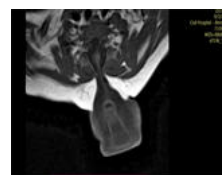
Cutaneous Signs	Dermal sinus	Tuft of hair	Nevus	Palpable mass	Dermal dimple	Capillary hemangioma	Total
No. of cases	3	2	8	16	3	3	35
%	8.57	5.71	22.8	45.71	8.57	8.57	100



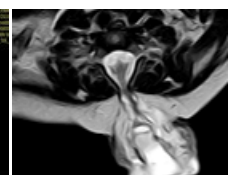
A



B



C



D

Figure 1. Myelomeningocele in cervicodorsal region. Sagittal T1WI (Fig.1A), Sagittal T2WI (Fig. 1B), Axial T1WI (Fig.1C) & Axial T2WI (Fig. 1D) show herniation of meninges, neural placode and CSF posteriorly into sac in cervicodorsal region.

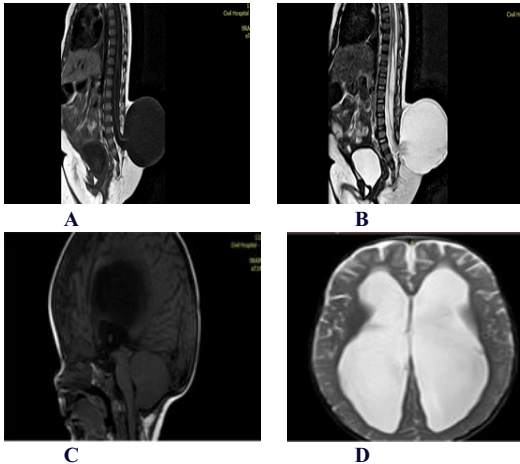


Figure 2. Chiari II malformation. Sagittal T1WI (Fig.2A) and Sagittal T2WI (Fig. 2B) show Myelomeningocele in lumbosacral region. Sagittal T1WI (Fig.1C) shows small sized posterior fossa with herniation of brainstem and cerebellar vermis into cervical spinal canal. Axial T2WI (Fig. 2D) shows hydrocephalus.

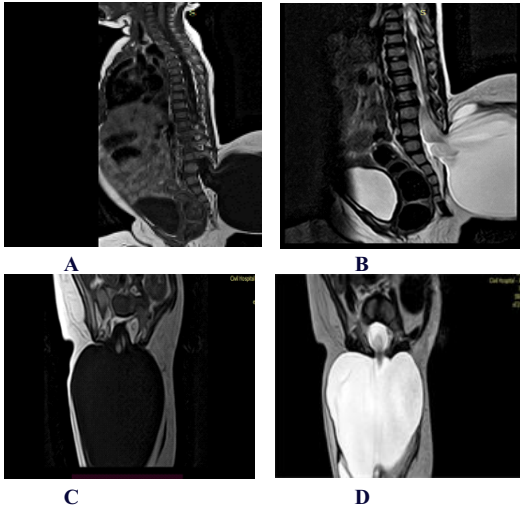


Figure 3. Lipomyelomeningocele. Sagittal T1WI (Fig.3A), Sagittal T2WI (Fig.3B), Axial T1WI (Fig.3C) & Axial T2WI (Fig.3D) show herniation of meninges, neural placode and CSF posteriorly into sac in lumbosacral region. Sac is covered by skin & subcutaneous fat.

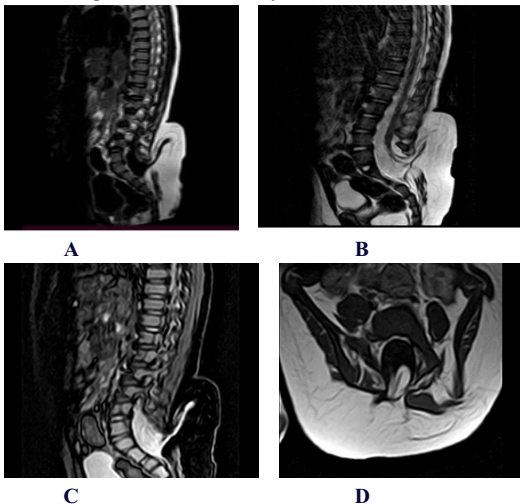


Figure 4. Lipomyelocele. Sagittal T1WI (Fig.4A), Sagittal T2WI (Fig. 4B), Sagittal STIR (Fig.4C) & Axial T1WI (Fig.4D) show

Lipomyelocele in lumbosacral region.

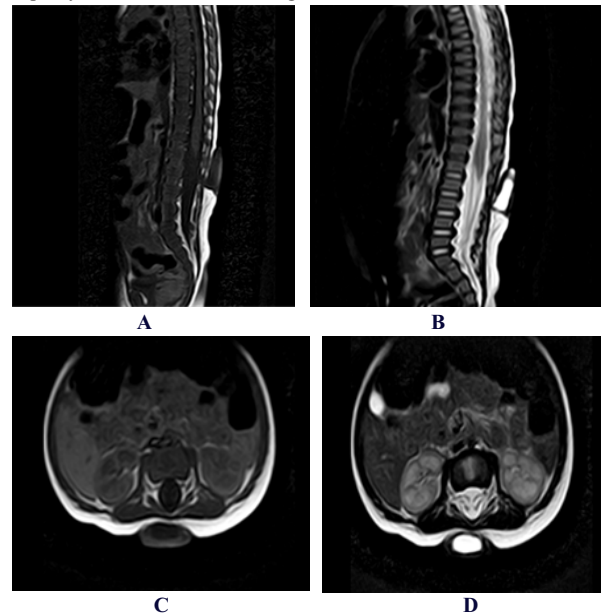


Figure 5. Meningocele. Sagittal T1WI (Fig.5A), Sagittal T2WI (Fig.5B), Axial T1WI (Fig.5C) & Axial T2WI (Fig.5D) show herniation of meninges and CSF posteriorly into sac in lumbar region. Sac is covered by skin.

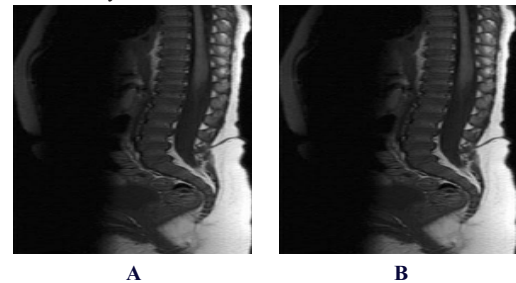


Figure 6. Dorsal dermal sinus. Sagittal T1WI (Fig.6A) & Sagittal T2WI (Fig.6B) show presence of linear hypointense tract in lumbar region in midline extending from skin into subcutaneous plane and muscular plane in oblique anteroinferior direction reaching upto posterior dural wall.

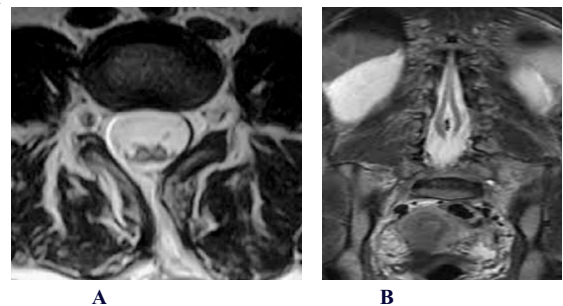


Figure 7. Diastematomyelia type 1. Axial T2WI (Fig.7A) and Coronal T2WI (Fig.7B) show splitting of cord into two hemicords separated by rigid osseous septum suggestive of type 1 diastematomyelia in lumbar region.

DISCUSSION:

According to the clinical-radiologic classification, SDs are categorized into two major groups: open SDs and closed SDs, depending on whether there is a skin defect overlying the abnormality. In open SDs, there is direct exposure of the neural tissue and meninges to the external environment. Open SD includes myelomeningocele, myelocele, hemimyelocele, and hemimyelomeningocele. Myelomeningocele accounts for approximately 99% cases of OSD while myelocele, hemimyelocele, and hemimyelomeningocele are distinctively rare. In closed SDs, the neural and meningeal tissues are covered by skin or subcutaneous tissue; therefore, there is no exposure of the placode.¹ Closed SDs are subdivided into two groups: those with

a subcutaneous mass and those without a subcutaneous mass. Closed SD with subcutaneous mass includes lipomyelocele, lipomyeloschisis, lipomyelomenigocele, myelocystocele & meningocele. Closed SDs lacking a subcutaneous mass can be further classified as simple dysraphic states and complex dysraphic states.^{2,3,5} Simple dysraphic states include filar/intradural lipoma, tight filum terminale & persistence of terminal ventricle. Complex dysraphic states include dorsal dermal sinus, diastematomyelia, caudal regression syndrome & limited dorsal myeloschisis.

All cases of open SD present at birth, while some cases of closed SD can present later in life. In our study, 93 patients were in age group of 0-10 yrs, while 7 patients were in age group of 11-20 yrs. All 7 patients of age group of 11-20 yrs were having closed SD. In our study, 45 patients were male & 55 were female.

According to literature, Myelomenigocele is the most common type of SD. In our study, most common SD was Myelomenigocele followed by Lipomyelomenigocele. In our study, majority of cases were involving lumbosacral spine.

MYELOMENIGOCELE:

Myelomenigocele [Figure 1] is clinically and radiologically defined by two main characteristics: (a) exposure of the neural placode to the environment with (b) expansion of the underlying subarachnoid space. Both protrude through the spina bifida, with elevation of the placode above the skin surface by expansion of the subarachnoid space in the midline of the back.^{2,6,7} Myelomenigocele is a neurosurgical emergency like all open SDs. It has a prevalence of approximately 0.6–1.0 per 1000 live births^{2,6,7}, and females are affected slightly more often than males.² The lower lumbar and upper sacral regions are the most frequently affected segments. Myelomenigocele is rare in the cervical and upper thoracic spine.

MYELOCELE AND MYELOSCHISIS:

Myelocele represents a rarer form of open SD in which the placode is exposed to the environment through a spina bifida, like in myelomenigocele, but without posterior expansion of the subarachnoid space.^{2,6,7} There is discontinuity of skin and subcutaneous tissue, with the placode exposed to the environment and forming the posterior wall of the spina bifida. The placode is flush with the skin surface (myelocele) or depressed (myeloschisis) because there is no expansion of the underlying subarachnoid space. The affected spinal cord segment anchors in the ventral wall of the placode. Nerve roots that originate from the ventral surface of the placode course anteriorly through the subarachnoid space of the spinal canal and go to the neural foramina.^{2,6,7,8,9,10}

HEMIMYELOMENIGOCELE & HEMIMYELOCELE:

Hemi-open SD is an extremely rare condition, defined as splitting of the spinal cord (diastematomyelia) in which one hemicord fails to neurulate (failure in primary neurulation process) and is therefore exposed to the environment. There are two types of hemi-open SD: hemimyelomenigocele occurs when there is dorsal expansion of the subarachnoid space that elevates the hemiplacode above the skin surface, and hemimyelocele occurs when the hemiplacode is flush with the skin surface.^{2,6,7,9}

CHIARI II MALFORMATION:

Chiari II malformation [Figure 2] can occur in all open SDs and can be considered a continuum of the malformation. The severity of the posterior fossa malformation is variable and can be explained by CSF leak through the SD in the amniotic sac, promoting underdevelopment of the fourth ventricle. The main imaging findings are small posterior fossa, herniation of the brainstem and cerebellar tonsils or vermis through the foramen magnum, dilatation of the supratentorial ventricular system, callosal dysgenesis, and tectal beaking.^{2,6,7,9,11}

LIPOMAS WITH DURAL DEFECT:

Lipomas with dural defect (LDDs) constitute a continuum of abnormalities (lipomyelomenigocele, lipomyelocele, and lipomyeloschisis) that share a common pathophysiologic process. They differ from each other by the position of the cord-lipoma interface, which is important information for the surgical approach.

LIPOMYELOMENIGOCELE:

Lipomyelomenigocele [Figure 3] is characterized by the combination of a subcutaneous lipoma with a posterior meningocele.⁶ MRI shows

enlargement of the spinal canal with expansion of the subarachnoid space. The low-lying spinal cord crosses into the meningocele and attaches to a subcutaneous lipoma. The cord-lipoma interface is located outside the vertebral canal and usually occurs off midline, with traction of the placode toward the lipoma on one side and meningeal herniation on the other side.

LIPOMYELOCELE AND LIPOMYEOSCHISIS:

These subtypes of closed SD share similar imaging findings and are characterized by a posterior neural arch defect (spina bifida), through which a lipomatous subcutaneous mass penetrates the spinal canal and attaches to the tethered cord.⁶ The spinal canal can be expanded depending on the size of the lipoma, but there is no evidence of meningeal herniation or expansion of the subarachnoid space. The distinguishing factor between these two conditions is the position of the cord-lipoma interface: at the level of the neural arches (lipomyelocele) [Figure 4] or within the spinal canal (lipomyeloschisis).

MENIGOCELE:

Meningocele [Figure 5] is a CSF hernia delineated by a dural and arachnoid lining through a posterior spina bifida. Meningoceles do not contain neural tissue, which explains the usually mild neurologic condition. These cystic formations are covered by soft tissue and skin and may manifest with alterations, such as cutaneous dystrophy, hemangioma, or tail-like protrusion.^{6,12}

MYELOCYSTOCELE:

Myelocystocele is defined as herniation of a hydrosyringomyelic cavity through the spina bifida into a meningocele. Myelocystocele can occur at any level of the spine. It is classified as terminal when located in the lumbosacral region or as nonterminal when it occurs in the cervical or thoracic segment.^{6,13,14}

INTRADURAL LIPOMA:

Intradural lipoma is a benign elongated lesion composed of adipose cells contained within the dural sac, unlike lipoma with dural defect (LDD).^{15,16} At MRI, intradural lipoma is depicted as a subpial lipomatous lesion lying between the folds of the placode. Large lipomas can displace the spinal cord and appear off midline. Rarely, it is seen as an intramedullary lesion or even as intramedullary lipomatosis.^{2,6,7,17}

LIPOMA OF FILUM TERMINALE:

At MRI, filar lipoma appears as a small lipomatous lesion in the filum terminale region with no communication with the medullary cone. It can be associated with other conditions, especially type II caudal agenesis syndrome or tethered cord syndrome.^{18,19}

DERMAL SINUS TRACT:

Dermal sinus tract (DST) or dorsal dermal sinus [Figure 6] is defined as a midline fistula lined by epithelium that connects the skin surface with the central nervous system or its meningeal membranes. MRI demonstrates a thin band, coursing through the subcutaneous tissue with an oblique and descending trajectory. It extends from the skin surface to the vertebral canal and is usually detected in the sagittal and axial planes. MRI can also depict associated malformations, such as ectodermal inclusion cysts.

DIASTEMATOMYELIA:

Diastematomyelia, a type of split-cord malformation⁶, is defined by division of the spinal cord into two hemicords, each covered by its own layer of pia mater and having its own central canal. It is divided into type I and type II. Differentiation between the two types of diastematomyelia depends on development of primitive streak tissue. In type I [Figure 7], the intervening primitive streak develops into bone or cartilage, creating a septum (radiologic mark) that separates the dural sac in two. In type II, the primitive streak is reabsorbed or forms a fibrous septum, with a single dural sac containing both hemicords.

CAUDAL REGRESSION SYNDROME:

Caudal regression syndrome (CRS), caudal regression sequence, or sacral agenesis²⁰ comprises a range of abnormalities in the lower half of the body, including lumbosacral agenesis, along with variable malformations in the lower limbs and genitourinary and gastrointestinal systems and pulmonary hypoplasia.

CONCLUSION:

Spinal dysraphisms (SDs) represent a heterogeneous group of

abnormalities that occur owing to derangements in the steps of the complex cascade of spinal embryology. Myelomeningocele is the most common type of spinal dysraphism. Open SDs typically manifest during the first year of life with majority of patients presenting with serious neurological symptoms. Closed SDs usually manifest as cutaneous stigmata and mild neurological symptoms in a later age group. MRI is the mainstay modality in use for SDs. MRI is safe to use in children due to lack of ionizing radiation. MRI allows for the delineation of the spinal cord, subarachnoid space, vertebral bodies, posterior elements, intervertebral discs & other soft tissues. MRI plays a pivotal role in diagnosis and presurgical evaluation of SDs. Therefore, knowledge of main imaging findings of these malformations is essential for the radiologist.

REFERENCES:

1. Reghunath A, Ghasi RG, Aggarwal A. Unveiling the tale of the tail: an illustration of spinal dysraphisms. *Neurosurg Rev* 2019. 10.1007/s10143-019-01215-z. Published online December 7, 2019.
2. Schwartz EC, Barkovich AJ. Congenital Anomalies of the Spine. In: Zinner S, Pecarich L, eds. *Pediatric neuroimaging*. 6th ed. Philadelphia, Pa: Wolters Kluwer, 2018; 1311–1377.
3. Dias MS, Walker ML. The embryogenesis of complex dysraphic malformations: a disorder of gastrulation? *Pediatr Neurosurg* 1992;18(5-6):229–253.
4. Kumar J, Afsal M, Garg A. Imaging spectrum of spinal dysraphism on magnetic resonance: a pictorial review. *World J Radiol* 2017;9(4):178–190.
5. Tortori-Donati P, Rossi A, Cama A. Spinal dysraphism: a review of neuroradiological features with embryological correlations and proposal for a new classification. *Neuroradiology* 2000;42(7):471–491.
6. Rossi A. Imaging in Spine and Spinal Cord Developmental Malformations. In: Barkhof F, Jäger HR, Thurnher MM, Rovira A, eds. *Clinical Neuroradiology: The ESNR Textbook*. Cham, Switzerland: Springer, 2018; 1609–1640.
7. Tortori-Donati P. Congenital Malformations of the Spine and Spinal Cord. In: Tortori-Donati P, Rossi A, eds. *Pediatric Neuroradiology*. Cham, Switzerland: Springer, 2005; 1551–1608.
8. Rossi A, Biancheri R, Cama A, Piatelli G, Ravegnani M, Tortori-Donati P. Imaging in spine and spinal cord malformations. *Eur J Radiol* 2004;50(2):177–200.
9. Kaufman BA. Neural tube defects. *Pediatr Clin North Am* 2004;51(2):389–419.
10. Parmar H, Patkar D, Shah J, Maheshwari M. Diastematomyelia with terminal lipomyelocystocele arising from one hemicoord: case report. *Clin Imaging* 2003;27(1):41–43.
11. Cama A, Tortori-Donati P, Piatelli GL, Fondelli MP, Andreussi L. Chiari complex in children: neuroradiological diagnosis, neurosurgical treatment and proposal of a new classification (312 cases). *Eur J Pediatr Surg* 1995;5(suppl 1):35–38.
12. Rufener SL, Ibrahim M, Raybaud CA, Parmar HA. Congenital spine and spinal cord malformations: pictorial review. *AJR Am J Roentgenol* 2010;194(3 suppl):S26–S37.
13. Muthukumar N. Terminal and nonterminal myelocystoceles. *J Neurosurg* 2007;107(2 suppl):87–97.
14. Awad T. Terminal Myelocystocele: A Rare Variant of Spinal Dysraphism—Case Series and Review of the Literature. *Egypt Spine J* 2016;17(1):28–33.
15. Shen SH, Ling JF, Chang FC, et al. Magnetic resonance imaging appearance of intradural spinal lipoma. *Zhonghua Yi Xue Za Zhi (Taipei)* 2001;64(6):364–368.
16. Pasalic I, Brgic K, Nemir J, Kolenc D, Njiric N, Mrak G. Intramedullary Spinal Cord Lipoma Mimicking a Late Subacute Hematoma. *Asian J Neurosurg* 2018;13(4):1282–1284.
17. Byrd SE, Harvey C, McLone DG, Darling CF. Imaging of terminal myelocystoceles. *J Natl Med Assoc* 1996;88(8):510–516.
18. Asma B, Dib O, Chahinez H, et al. Imaging findings in spinal dysraphisms. EPoster C-1516, 2017 European Congress of Radiology. <https://doi.org/10.1594/ecr2017/C-1516>. Published 2017. Accessed April 2, 2020.
19. Cools MJ, Al-Holou WN, Stetler WR Jr, et al. Filum terminale lipomas: imaging prevalence, natural history, and conus position. *J Neurosurg Pediatr* 2014;13(5):559–567.
20. Heuser CC, Hulinky RS, Jackson GM. Caudal Regression Syndrome. In: Copel JA, D'Alton ME, Feltovich H, et al., eds. *Obstetric Imaging: Fetal Diagnosis and Care*. 2nd ed. Philadelphia, Pa: Elsevier, 2018; 291–294.